

# On Departures From a Power Law in the Galaxy Correlation Function

Idit Zehavi<sup>1,2</sup>, David H. Weinberg<sup>3</sup>, Zheng Zheng<sup>3</sup>, Andreas A. Berlind<sup>1,5</sup>, Joshua A. Frieman<sup>1,4</sup>, Roman Scoccimarro<sup>5</sup>, Ravi K. Sheth<sup>6</sup>, Michael R. Blanton<sup>5</sup>, Max Tegmark<sup>7</sup>, Houjun J. Mo<sup>8</sup>, Neta A. Bahcall<sup>9</sup>, Jon Brinkmann<sup>10</sup>, Scott Burles<sup>11</sup>, Istvan Csabai<sup>12,13</sup>, Masataka Fukugita<sup>14</sup>, James E. Gunn<sup>9</sup>, Don Q. Lamb<sup>1</sup>, Jon Loveday<sup>15</sup>, Robert H. Lupton<sup>9</sup>, Avery Meiksin<sup>16</sup>, Jeffrey A. Munn<sup>17</sup>, Robert C. Nichol<sup>18</sup>, David Schlegel<sup>9</sup>, Donald P. Schneider<sup>19</sup>, Mark SubbaRao<sup>1</sup>, Alexander S. Szalay<sup>12</sup>, Alan Uomoto<sup>12</sup>, and Donald G. York<sup>1</sup> (for the SDSS Collaboration)

## ABSTRACT

We measure the projected correlation function  $w_p(r_p)$  from the Sloan Digital Sky Survey for a flux-limited sample of 118,000 galaxies and for a volume-limited subset of 22,000 galaxies with absolute magnitude  $M_r < -21$ . Both correlation functions show

---

<sup>1</sup>Astronomy and Astrophysics Department, University of Chicago, Chicago, IL 60637, USA

<sup>2</sup>Steward Observatory, University of Arizona, 933 N. Cherry Ave., Tucson, AZ 85721, USA

<sup>3</sup>Department of Astronomy, Ohio State University, Columbus, OH 43210, USA

<sup>4</sup>Fermi National Accelerator Laboratory, P.O. Box 500, Batavia, IL 60510, USA

<sup>5</sup>Department of Physics, New York University, 4 Washington Place, New York, NY 10003, USA

<sup>6</sup>University of Pittsburgh, Department of Physics and Astronomy, 3941 O'Hara Street, Pittsburgh, PA 15260, USA

<sup>7</sup>Department of Physics, University of Pennsylvania, Philadelphia, PA 19101, USA

<sup>8</sup>Max-Planck-Institute for Astrophysics, Karl-Schwarzschild-Strasse 1, D-85741 Garching, Germany

<sup>9</sup>Princeton University Observatory, Peyton Hall, Princeton, NJ 08544, USA

<sup>10</sup>Apache Point Observatory, P.O. Box 59, Sunspot, NM 88349, USA

<sup>11</sup>Center for Space Research, Massachusetts Institute of Technology, 77 Massachusetts Avenue, Cambridge, MA 02139, USA

<sup>12</sup>Department of Physics and Astronomy, The Johns Hopkins University, 3701 San Martin Drive, Baltimore, MD 21218, USA

<sup>13</sup>Department of Physics, Eötvös University, Budapest, Pf. 32, Hungary, H-1518

<sup>14</sup>Institute for Cosmic Ray Research, University of Tokyo, Kashiwa 277-8582, Japan

<sup>15</sup>Sussex Astronomy Centre, University of Sussex, Falmer, Brighton BN1 9QJ, UK

<sup>16</sup>Institute for Astronomy, The University of Edinburgh, Mayfield Road, Edinburgh, EH9 3JZ, UK

<sup>17</sup>U.S. Naval Observatory, Flagstaff Station, P.O. Box 1149, Flagstaff, AZ 86002, USA

<sup>18</sup>Department of Physics, 5000 Forbes Avenue, Carnegie Mellon University, Pittsburgh, PA 15213, USA

<sup>19</sup>Department of Astronomy and Astrophysics, The Pennsylvania State University, University Park, PA 16802, USA

subtle but systematic departures from the best-fit power law, in particular a change in slope at  $r_p \sim 1 - 2 h^{-1}$  Mpc. These departures are stronger for the volume-limited sample, which is restricted to relatively luminous galaxies. We show that the inflection point in  $w_p(r_p)$  can be naturally explained by contemporary models of galaxy clustering, according to which it marks the transition from a large scale regime dominated by galaxy pairs in separate dark matter halos to a small scale regime dominated by galaxy pairs in the same dark matter halo. For example, given the dark halo population predicted by an inflationary cold dark matter scenario, the projected correlation function of the volume-limited sample can be well reproduced by a model in which the mean number of  $M_r < -21$  galaxies in a halo of mass  $M > M_1 = 4.74 \times 10^{13} h^{-1} M_\odot$  is  $\langle N \rangle_M = (M/M_1)^{0.89}$ , with 75% of the galaxies residing in less massive, single-galaxy halos, and simple auxiliary assumptions about the spatial distribution of galaxies within halos and the fluctuations about the mean occupation. This physically motivated model has the same number of free parameters as a power law, and it fits the  $w_p(r_p)$  data better, with a  $\chi^2/\text{d.o.f.} = 0.93$  compared to 6.12 (for 10 degrees of freedom, incorporating the covariance of the correlation function errors). Departures from a power-law correlation function encode information about the relation between galaxies and dark matter halos. Higher precision measurements of these departures for multiple classes of galaxies will constrain galaxy bias and provide new tests of the theory of galaxy formation.

*Subject headings:* cosmology: observations — cosmology: theory — galaxies: distances and redshifts — galaxies: fundamental parameters — galaxies: statistics — large-scale structure of universe

## 1. Introduction

One of the longest standing quantitative results in the study of galaxy clustering is the power-law form of the two-point correlation function  $\xi(r)$  (Totsuji & Kihara 1969; Peebles 1974; Gott & Turner 1979). For many years this result rested mainly on the angular correlation function of imaging catalogs, measured with steadily increasing precision and dynamic range. More recently, analyses of the projected correlation function  $w_p(r_p)$  in large galaxy redshift surveys have confirmed that the real space galaxy correlation function is close to a power law on small scales (e.g., Davis & Peebles 1983; Fisher et al. 1994; Marzke et al. 1995; Jing, Mo, & Börner 1998; Norberg et al. 2001; Jing, Börner, & Suto 2002; Zehavi et al. 2002, hereafter Z02). The angular correlation function (as well as the redshift-space correlation function) breaks below a power law at large scales ( $\gtrsim 10 - 20 h^{-1}$  Mpc; Groth & Peebles 1977; Maddox et al. 1990; Jing, Börner, & Suto 2002), and there are hints of a “shoulder” in  $\xi(r)$  at scales of several  $h^{-1}$  Mpc (Dekel & Aarseth 1984; Guzzo et al. 1991; Calzetti, Giavalisco, & Meiksin 1992; Baugh 1996; Gaztañaga & Juszkiewicz 2001; Gaztañaga 2002; Hawkins et al. 2003). There have also been some hints of departures from a power law at smaller scales (e.g., Connolly et al. 2002), but the significance of these has been difficult to

evaluate for two reasons: they are usually measured in the angular correlation function and are thus integrated over a wide range of galaxy luminosities and redshifts, and the statistical errors in correlation function estimates are themselves correlated in a complex way.

It has become increasingly clear that leading cosmological models do not predict a power-law  $\xi(r)$  for the dark matter. For the  $\Lambda$ CDM model (inflationary cold dark matter with a cosmological constant), the matter correlation function rises above a best-fit power law on scales  $r \lesssim 1 h^{-1}$  Mpc and falls below it again on scales  $r \lesssim 0.2 h^{-1}$  Mpc (Jenkins et al. 1998, and references therein;  $h \equiv H_0/100 \text{ km s}^{-1} \text{ Mpc}^{-1}$ ). Semi-analytic and hydrodynamic simulation models of galaxy formation, and high resolution N-body simulations that identify galaxies with sub-halos inside larger virialized objects, predict a scale-dependent bias that makes the galaxy correlation function much closer to the observed power law, a significant success of these galaxy formation models in the context of  $\Lambda$ CDM (Colín et al. 1999; Kauffmann et al. 1999; Pearce et al. 1999; Benson et al. 2000; Cen & Ostriker 2000; Somerville et al. 2001; Yoshikawa et al. 2001; Weinberg et al. 2004). However, while the general form of this bias can be understood qualitatively in terms of the physics of galaxy assembly (Kauffmann, Nusser, & Steinmetz 1997; Kauffmann et al. 1999; Benson et al. 2000; Berlind et al. 2003), the emergence of a power law  $\xi(r)$  is largely fortuitous. In particular, there is a transition from a large scale regime in which pairs come from separate dark matter halos to a small scale regime in which pairs come from the same halo, and a power law correlation function requires coincidental alignment of these two terms.<sup>1</sup> Thus, the best contemporary models of galaxy clustering predict that sufficiently high precision measurements of the correlation function should, eventually, show departures from a power law.

Here we present measurements of  $w_p(r_p)$  from the main galaxy redshift sample of the Sloan Digital Sky Survey (SDSS; York et al. 2000). The correlation function of the flux-limited sample shows small but systematic deviations from a power law. When we measure  $w_p(r_p)$  for a volume-limited sample of relatively luminous galaxies ( $M_r < -21$ ,  $L \gtrsim 1.5L_*$ ), we find deviations of similar form and larger amplitude. In addition to establishing the existence of these deviations, a second goal of this paper is to introduce new techniques for modeling the projected correlation function in terms of the relation between galaxies and halos, extending the approach of Jing, Mo, & Börner (1998) and Jing, Börner, & Suto (2002) and building on theoretical work by Ma & Fry (2000), Peacock & Smith (2000), Seljak (2000), Scoccimarro et al. (2001), and Berlind & Weinberg (2002). We concentrate our modeling effort on the volume-limited sample, since it constitutes a well defined class of galaxies. We show that the departures of the measured  $w_p(r_p)$  from a power law can be naturally explained by the predicted transition from a 2-halo regime on large scales to a 1-halo regime on small scales. We will examine the dependence of  $w_p(r_p)$  on galaxy luminosity and color, and the implications of this dependence for galaxy-halo relations, in a separate paper (I. Zehavi et

---

<sup>1</sup>Throughout this paper we use the term “halo” to refer to a gravitationally bound structure with overdensity  $\rho/\bar{\rho} \sim 200$ , so an occupied halo may host a single luminous galaxy, a group of galaxies, or a cluster. Higher overdensity concentrations around individual galaxies of a group or cluster constitute, in this terminology, halo substructure or “sub-halos.”

al., in preparation).

## 2. Observations and Analysis

The SDSS uses a mosaic CCD camera (Gunn et al. 1998) to image the sky in five photometric bandpasses (Fukugita et al. 1996), denoted  $u$ ,  $g$ ,  $r$ ,  $i$ ,  $z$ .<sup>2</sup> After astrometric calibration (Pier et al. 2003), photometric data reduction (R. H. Lupton et al., in preparation; see Lupton et al. 2001 and Stoughton et al. 2002 for summaries), and photometric calibration (Hogg et al. 2001; Smith et al. 2002), galaxies are selected for spectroscopic observations using the algorithm described by Strauss et al. (2002). To a good approximation, the main galaxy sample consists of all galaxies with  $r$ -band apparent magnitude  $r < 17.77$ ; the analysis in this paper does not include galaxies in the luminous red galaxy sample described by Eisenstein et al. (2001). Spectroscopic observations are performed with a pair of fiber-fed CCD spectrographs (A. Uomoto et al., in preparation), with targets assigned to spectroscopic plates by an adaptive tiling algorithm (Blanton et al. 2003a). An important operational constraint is that no two fibers on the same plate can be closer than 55'' (a.k.a fiber collisions, affecting  $\sim 7\%$  of the galaxies). Spectroscopic data reduction and redshift determination are performed by automated pipelines (D. J. Schlegel et al., in preparation; J. A. Frieman et al., in preparation), with rms galaxy redshift errors  $\sim 30 \text{ km s}^{-1}$ .

The clustering measurements in this paper are based on a subset of the SDSS galaxy redshift data with well characterized completeness, known as Large Scale Structure `sample10`, which is described in detail by Blanton et al. (2003c). LSS `sample10` is based on data obtained prior to April 2002, and it contains 144,609 main sample galaxies. The radial selection function incorporates the luminosity evolution model of Blanton et al. (2003c) and the improved K-corrections of Blanton et al. (2003b, using `kcorrect v1_11`). We K-correct the observed frame magnitudes in the SDSS bands to rest frame magnitudes for those bands blueshifted by  $z = 0.1$ , so that the K-correction is trivial for a galaxy at  $z = 0.1$  (near the median redshift of the survey). The one photometric quantity of importance to this paper is the absolute magnitude in the redshifted  $r$  band, which we compute for  $h = 1$  and denote  $M_{0.1r}$  (so that the true absolute magnitude is  $M_{0.1r} + 5 \log h$ .) We will focus most of our attention on a volume-limited galaxy sample with  $M_{0.1r} < -21$ , a threshold that is 0.56 magnitudes brighter than the characteristic Schechter (1976) function luminosity  $M_{0.1r}^*$  found by Blanton et al. (2003c). For all absolute-magnitude and distance calculations, we adopt a cosmological model with  $\Omega_m = 0.3$  and  $\Omega_\Lambda = 0.7$ .

Our methods for measuring the galaxy correlation function are essentially the same as those of Z02, to which we refer the reader for a detailed description and tests. In brief, we create random catalogs using the survey angular selection function and the radial selection function appropriate

---

<sup>2</sup>Fukugita et al. (1996) actually define a slightly different system, denoted  $u'$ ,  $g'$ ,  $r'$ ,  $i'$ ,  $z'$ , but SDSS magnitudes are now referred to the native filter system of the 2.5-m survey telescope, for which the bandpass notation is unprimed.

to the galaxy sample under consideration. We calculate  $\xi(r_p, \pi)$ , the correlation function as a function of separation perpendicular ( $r_p$ ) and parallel ( $\pi$ ) to the line-of-sight, by counting data-data, data-random, and random-random pairs and using the Landy & Szalay (1993) estimator. We then compute the projected correlation function  $w_p(r_p)$ ,

$$w_p(r_p) = 2 \int_0^{\pi_{\max}} \xi(r_p, \pi) d\pi. \quad (1)$$

We adopt  $\pi_{\max} = 4000 \text{ km s}^{-1} = 40 h^{-1} \text{ Mpc}$ , which is large enough to include essentially all significant signal at the values of  $r_p$  of interest here ( $0.1 h^{-1} \text{ Mpc} < r_p < 20 h^{-1} \text{ Mpc}$ ) while suppressing noise from uncorrelated structure at very large line-of-sight separations. We account for spectroscopic fiber collisions by assigning to each “collided” (and thus unobserved) galaxy the same redshift as the observed galaxy responsible for the collision. The main advances relative to Z02 are the much larger data sample, the improved model of the radial selection function, and the improved error estimates discussed below.

Figure 1a shows the projected correlation function  $w_p(r_p)$  of a flux-limited subset of `sample10`. We restrict this subset to galaxies in the absolute-magnitude range  $-19 > M_{0.1r} > -22$  and the redshift range  $0.02 < z < 0.16$ , so that we avoid galaxies at the extremes of the luminosity distribution and minimize the effect of redshift evolution within the sample. Note, however, that the sample is not volume-limited, so that not all galaxies within the absolute-magnitude limits can be seen over the full redshift range. With our adopted redshift, absolute-magnitude, and angular limits, the flux-limited catalog contains 118,149 galaxies. In Figure 1a, the statistical error bars on the data points are estimated via the jackknife resampling procedure used by Z02. We define 104 geometrically contiguous subsamples of the full data set, each covering approximately 20 square degrees on the sky, then estimate error bars from the total dispersion among the 104 jackknife samples that are created by omitting each of these subsamples in turn (Z02, eq. 7).

The integration over line-of-sight separations makes  $w_p(r_p)$  independent of redshift-space distortions. In this respect, it resembles the angular correlation function  $w(\theta)$ , but because  $w_p(r_p)$  makes use of the known redshifts of each pair of galaxies, it is a much more sensitive measure (for a given number of galaxies) of the real space correlation function  $\xi(r)$  (Davis & Peebles 1983; Hamilton & Tegmark 2002). The general relation between  $w_p(r_p)$  and  $\xi(r)$  is

$$w_p(r_p) = 2 \int_0^\infty \xi \left[ (r_p^2 + y^2)^{1/2} \right] dy, \quad (2)$$

from which one can see that a power-law  $\xi(r)$  projects into a power-law  $w_p(r_p)$ . The solid line in Figure 1a shows a power-law fit to the  $w_p(r_p)$  data points, corresponding to a real space correlation function  $\xi(r) = (r/5.77 h^{-1} \text{ Mpc})^{-1.80}$ . Statistical errors in the correlation function are strongly correlated because each coherent structure contributes pairs at many different separations, and the solid-line fit utilizes the full covariance matrix estimated by jackknife resampling. If we ignore the error correlations and use only the diagonal elements of the covariance matrix, we obtain the slightly shallower power law shown by the dotted line, which corresponds to  $\xi(r) = (r/5.91 h^{-1} \text{ Mpc})^{-1.78}$ .

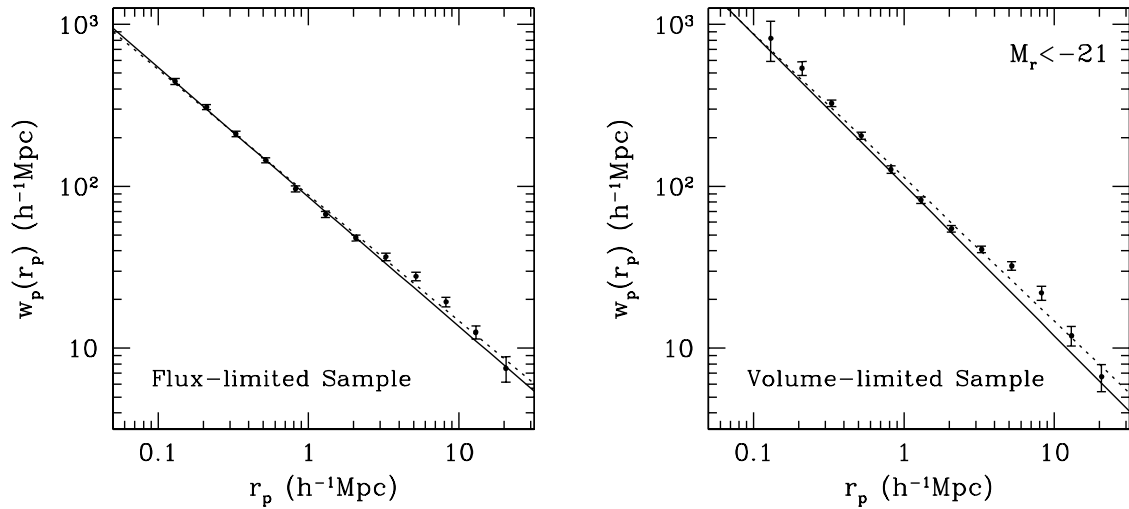


Fig. 1.— Projected correlation function  $w_p(r_p)$  for the flux-limited redshift sample (left) and the volume-limited subset of galaxies with  $M_{0.1r} < -21$  (right). For the flux-limited sample, error bars and their covariance matrix are estimated by jackknife resampling of the data set, while for the volume-limited sample they are estimated from mock catalogs as described in the text. In each panel, solid lines show maximum-likelihood power-law fits that incorporate the full error covariance matrix, and dotted lines show least-squares fits that ignore the error correlations.

While the data points in Figure 1a lie close to the best-fit power laws, they do not scatter randomly above and below. Instead, they criss-cross the fits, and they have a steeper logarithmic slope at  $0.5 h^{-1} \text{ Mpc} \lesssim r \lesssim 1.5 h^{-1} \text{ Mpc}$  and a shallower slope at  $1.5 h^{-1} \text{ Mpc} \lesssim r \lesssim 4 h^{-1} \text{ Mpc}$ . The  $\chi^2$  of the fit, estimated using the jackknife covariance matrix, is 31.8 for ten degrees of freedom (12 data points minus 2 parameters), which suggests that these departures are statistically significant. (Even though the data points are correlated, it is correct to count one degree of freedom per data point because we use the full covariance matrix in evaluation of  $\chi^2$ .) However, the physical implications of these departures are difficult to assess because galaxy clustering is known to depend on luminosity (Norberg et al. 2001; Z02, and references therein), and the flux-limited sample contains a different mix of galaxies at different redshifts and does not represent the clustering of any well defined class. Furthermore, while the tests in Z02 (and tests that we have conducted subsequently) show that the jackknife method yields reasonable estimates of the error covariance matrix on average, statistical noise in these estimates can lead to an inaccurate inverse matrix and consequently inaccurate  $\chi^2$  estimates.

To address both of these problems, we measure the projected correlation function of a volume-limited subset of galaxies with  $M_{0.1r} < -21$  and the same redshift range  $0.02 < z < 0.16$ . All 21,659 galaxies in this subset are luminous enough to be seen over the full redshift range. To obtain low noise estimates of the covariance matrix, we now create 100 mock catalogs with the same geometry, completeness as a function of sky position, and galaxy number density as this volume-limited sample, using the PTHalos method of Scoccimarro & Sheth (2002). The input parameters for these catalogs are chosen based on the model described in §4, with the consequence that the average  $w_p(r_p)$  of these mock catalogs is close to the observed value. Thus, this covariance matrix should be appropriate for fitting models to these data and for assessing the statistical acceptability of fits. To account for the small residual mismatch between the mock catalog and observed  $w_p(r_p)$ , we rescale covariance matrix elements  $C_{ij}$  by the ratio of the observed and mock  $w_p(r_{p,i})w_p(r_{p,j})$ , in effect assuming that the mock catalogs most accurately predict the fractional rather than absolute errors in  $w_p(r_p)$ . However, our conclusions would be no different if we did not apply this scaling.

Figure 1b shows  $w_p(r_p)$  of the  $M_{0.1r} < -21$  sample, with error bars on the data points representing the square root of the diagonal elements of the covariance matrix estimated from the mock catalogs. The dotted line shows a power-law fit that incorporates only these diagonal elements, while the solid line shows a maximum-likelihood fit that uses the full covariance matrix. The corresponding real space correlation functions are  $\xi(r) = (r/6.40 h^{-1} \text{ Mpc})^{-1.89}$  and  $\xi(r) = (r/5.91 h^{-1} \text{ Mpc})^{-1.93}$ , respectively. Since the error correlations for the large scale data points are particularly strong, the full maximum-likelihood fit puts more effective weight on the data points at smaller scales, yielding a steeper power law.

Relative to the power-law fits, the data points in Figure 1b show the same systematic departures seen for the flux-limited sample but in exaggerated form, especially the marked change in slope at  $r_p \approx 2 h^{-1} \text{ Mpc}$ . We find deviations of similar form for most other volume-limited SDSS samples (I.

Zehavi et al., in preparation), but the deviations are stronger for the relatively luminous galaxies selected by the  $M_{0.1r} < -21$  threshold. Deviations of similar form are seen in the projected correlation function of the 2dF Galaxy Redshift Survey (2dFGRS), as shown by Hawkins et al. (2003, see their Figure 9), who comment that the deviation “probably is a real feature,” though they do not assess the significance quantitatively or discuss the physical interpretation in detail. The existence of these deviations in flux- and volume-limited subsets of the  $r$ -band limited SDSS and in the independent,  $b_J$ -band limited 2dFGRS demonstrates their observational robustness, though their magnitude does depend on galaxy luminosity and color.

The  $\chi^2$  for the solid-line fit in Figure 1b, based on the full covariance matrix and thus accounting for the correlation of errors, is 61.2 for 10 degrees of freedom, or  $\chi^2/\text{d.o.f.} = 6.12$ . (A similar fit with  $\chi^2/\text{d.o.f.} = 4.37$  is obtained with the jackknife covariance matrix.) We now show that a physically motivated model with the same number of free parameters provides a significantly better fit to the data.

### 3. Modeling the Correlation Function

To model  $w_p(r_p)$  in a way that accounts for non-linear cosmological evolution and the potentially complex relation between galaxies and mass, we adopt the general framework of the “halo occupation distribution” (HOD) and use a modified form of the calculational methods introduced by Ma & Fry (2000), Peacock & Smith (2000), Seljak (2000), Scoccimarro et al. (2001), and Berlind & Weinberg (2002). The HOD framework characterizes galaxy “bias” in terms of the probability  $P(N|M)$  that a halo of virial mass  $M$  contains  $N$  galaxies of a specified class, together with additional prescriptions that specify the relative distributions of galaxies and dark matter within halos. In addition to allowing us to understand the power law deviations found above, HOD modeling transforms  $w_p(r_p)$  measurements into the language of contemporary cosmological models and galaxy formation theories, which respectively predict the properties of the dark halo population (e.g., Press & Schechter 1974; Mo & White 1996; Sheth, Mo, & Tormen 2001; Jenkins et al. 2001) and the occupation statistics of galaxies (e.g., Kauffmann et al. 1997; Kauffmann et al. 1999; Benson et al. 2000; Somerville et al. 2001; White, Hernquist, & Springel 2001; Yoshikawa et al. 2001; Berlind et al. 2003; Kravtsov et al. 2004). While power law fits to correlation functions are more familiar, we consider the HOD fitting approach adopted here to be more physically natural, in addition to providing a better description of the data. Magliocchetti & Porciani (2003) have recently applied a similar approach to interpretation of clustering data from the 2dFGRS.

We start with the halo population predicted by a  $\Lambda$ CDM model, with parameters  $\Omega_m = 0.3$ ,  $\Omega_\Lambda = 0.7$ ,  $h = 0.7$ ,  $n = 1$ ,  $\sigma_8 = 0.9$ , using the Efstathiou, Bond, & White (1992) form of the CDM transfer function with parameter  $\Gamma = 0.21$ . These choices provide a reasonable match to a wide variety of cosmological observations, including the shapes of the 2dFGRS and SDSS galaxy power spectra at large scales where the bias is expected to be scale-independent (Percival et al. 2001; Tegmark et al. 2004). We compute the galaxy correlation function  $\xi(r)$  as a sum of two

terms, one representing pairs of galaxies that reside within the same dark matter halo, the other representing pairs in separate halos. We obtain the projected correlation function  $w_p(r_p)$  from  $\xi(r)$  via equation (2) (with the same upper limit of  $40 h^{-1}$  Mpc as in the measurements).

The 1-halo term is obtained by integrating over the Jenkins et al. (2001) halo mass function, weighting each halo of mass  $M$  by the mean number of galaxy pairs  $\langle N(N-1) \rangle_M$ . We assume that each dark halo has an NFW profile (Navarro, Frenk, & White 1996) with  $c(M) = 11(M/M_*)^{-0.13}$  (Bullock et al. 2001), where  $c$  is the NFW halo concentration parameter and  $M_* = 1.07 \times 10^{13} h^{-1} M_\odot$  is the non-linear mass scale for our adopted cosmological parameters.<sup>3</sup> Motivated by hydrodynamic simulation results (White, Hernquist, & Springel 2001; Berlind et al. 2003), we assume that the first galaxy in each occupied halo resides at the halo center-of-mass and that additional “satellite” galaxies trace the dark matter distribution; similar assumptions are standard practice in the HOD papers cited above and in galaxy clustering predictions based on N-body simulations with halos populated according to semi-analytic models (Kauffmann et al. 1997; Kauffmann et al. 1999; Benson et al. 2000; Somerville et al. 2001). We calculate the distribution of pair separations within each halo — the function  $F'(x)$  in equation (11) of Berlind & Weinberg (2002) — by Monte Carlo sampling of NFW halo realizations, assuming that the halos are spherical.

The 2-halo term is essentially the matter correlation function multiplied by the appropriately weighted halo bias factor (Sheth, Mo, & Tormen 2001; an improvement on earlier results by Mo & White 1996), with convolution to represent finite size of halos, and is calculated in Fourier space. Relative to Seljak (2000) and Scoccimarro et al. (2001), there are three significant changes in our calculation of the two-halo term. First, instead of the linear theory matter correlation function we use the non-linear correlation function, and make use of the non-linear power spectrum given by Smith et al. (2003). Second, we approximately incorporate the effects of halo exclusion by including in the 2-halo term at separation  $r$  only those halos whose virial radii are  $R_{\text{vir}} \leq r/2$  (similar to Takada & Jain 2003). Third, we incorporate scale dependence of the halo bias factor on non-linear scales, using an empirical formula  $b_h^2(M, r) = [1 + 0.2\xi_m(r)]^{-0.5} b_{h,\text{lin}}^2(M)$  obtained by matching the halo correlation functions of the GIF  $\Lambda$ CDM simulation (Jenkins et al. 1998). Here  $\xi_m(r)$  is the non-linear matter correlation function, and  $b_{h,\text{lin}}(M)$  is the large scale bias factor given by Sheth, Mo, & Tormen (2001) for halos of mass  $M$ . The ratio of the non-linear  $\xi_m(r)$  to the linear theory  $\xi(r)$  is  $\sim 0.75 - 0.8$  on scales of several  $h^{-1}$  Mpc, so it is essential to use the former when modeling data with the precision of the SDSS measurements. Once the non-linear  $\xi_m(r)$  is used, it is essential to account for halo exclusion and scale-dependent bias to obtain acceptable results on small scales. We present a test of the accuracy of our analytic approximation in the Appendix, demonstrating that it is adequate to our purposes in this paper.

For the halo occupation distribution itself, we adopt a simple model loosely motivated by

---

<sup>3</sup>We use  $c(M_*) = 11$  rather than 9 to account for our definition of halos as enclosing a sphere of mean overdensity 200, instead of the value 340 used by Bullock et al. (2001). We choose 200, in turn, because this definition more nearly corresponds to the one used in estimating the halo mass function.

results from smoothed particle hydrodynamic (SPH) simulations and semi-analytic calculations, e.g., the models of Kauffmann et al. (1997) and Benson et al. (2000), the fits of the Kauffmann et al. (1999) models by Seljak (2000) and Scoccimarro et al. (2001), the SPH results of White, Hernquist, & Springel (2001) and Yoshikawa et al. (2001), and the detailed comparison between SPH and semi-analytic predictions by Berlind et al. (2003). We assume that the mean occupation in halos of mass  $M \geq M_1$  is a power law,  $\langle N \rangle_M = (M/M_1)^\alpha$ , and that halos in the mass range  $M_{\min} < M < M_1$  contain a single galaxy above the luminosity threshold. The theoretical models cited above predict that the width of the distribution  $P(N|\langle N \rangle)$  at fixed halo mass is substantially narrower than a Poisson distribution when the mean occupation is low, making the mean number of pairs  $\langle N(N-1) \rangle_M$  lower than the Poisson expectation  $\langle N \rangle^2$ . This suppression of pairs in low mass halos has an important influence on the predicted correlation function. For our baseline model, we assume that the actual occupation for a halo of mass  $M$  is one of the two integers bracketing  $\langle N \rangle_M$ , though we will discuss some alternative cases in §4 below. As noted earlier, we assume that the first galaxy in any halo resides at the center of mass and that any remaining galaxies trace the dark matter within the halo. For given values of  $\alpha$  and  $M_1$ , we choose the value of  $M_{\min}$  to match the observed number density of  $M_{0.1r} < -21$  galaxies,  $n = 9.9 \times 10^{-4} h^3 \text{Mpc}^{-3}$ . Thus, there are two parameters ( $\alpha$  and  $M_1$ ) that can be varied to fit the correlation function. Of course there are many other parameters required to describe the cosmological model, the concentration-mass relation, and so forth, but all of these were chosen based on independent observational or theoretical considerations; we made our default choices before starting to model  $w_p(r_p)$  and did not adjust any of them in order to fit the data.

Our assumptions about the form of the HOD are restrictive and are unlikely to be exactly correct. However, they are reasonably motivated by current theoretical models, and they yield a 2-parameter description that can be fairly well constrained by  $w_p(r_p)$  measurements. The assumption that  $\langle N \rangle_M$  is flat between  $M_{\min}$  and  $M_1$  is clearly artificial, but because halos with  $M < M_1$  do not contribute to the 1-halo term of  $\xi(r)$ , our results are insensitive to the form of  $\langle N \rangle_M$  in this “single occupancy” regime; we have confirmed this expectation by considering alternative forms for  $\langle N \rangle_M$  in the range where  $\langle N \rangle < 1$ . The important quantity is the overall fraction of galaxies in halos with  $M < M_1$ , since this directly affects the normalization of the 1-halo term. Our modeling approach is similar in spirit to the “conditional luminosity function” studies of Yang, Mo, & van den Bosch (2003) and van den Bosch, Mo, & Yang (2003), but here we focus on luminosities  $M_{0.1r} < -21$  instead of simultaneously modeling the luminosity function and luminosity-dependent clustering, and we use the full correlation function  $w_p(r_p)$  as a constraint instead of the correlation length  $r_0$  alone. When other clustering measurements such as higher order correlations and the group multiplicity function are included, it is possible to constrain HOD models with much more freedom, and to simultaneously constrain the cosmological model (Berlind & Weinberg 2002; Z. Zheng & D. H. Weinberg, in preparation). We leave this effort to future work, when a wider range of complementary measurements are available.

Figure 2 illustrates the behavior of the real space galaxy correlation function  $\xi(r)$  for varying

choices of the model parameters  $M_1$  and  $\alpha$ . For each combination, the value of  $M_{\min}$  is chosen by matching the observed number density of  $M_{0.1r} < -21$  galaxies. Figure 2a shows the effect of varying  $\alpha$  and Figure 2b the effect of varying  $M_1$ . The central model in each panel has the parameters that yield the best fit to the  $w_p(r_p)$  data points of Figure 1, as we discuss in §4.

For the central model, Figure 2 plots the 1-halo and 2-halo contributions to  $\xi(r)$  in addition to the total. For other models, only the 1-halo terms and the total are shown; the 2-halo terms are similar but not identical to that of the central model. The 1-halo terms have a nearly power-law form at small scales, but they cut off fairly steeply at separations approaching the virial diameter of large halos, a consequence of the rapidly falling halo mass function. On large scales, the 2-halo term traces the shape of the matter correlation function, then it flattens and cuts off at  $r \sim 1-2 h^{-1} \text{ Mpc}$  as a consequence of halo exclusion and the scale-dependent halo bias described above. For higher  $\alpha$  or lower  $M_1$ , a larger fraction of galaxies reside in massive, high-occupancy halos with large virial radii, so the 1-halo term has higher amplitude and extends to larger  $r$ . Regardless of the specific parameter values, the transition from the 2-halo regime to the 1-halo regime represents a transition from a function that is flattening and cutting off to a function that is rising steeply. Thus, these models generically predict a change in the slope of the correlation function at scales comparable to the virial diameters of large halos. The strength and location of this break depend on the relative fractions of galaxies in high and low mass halos.

#### 4. Fitting the Observations

Figure 3 compares the observed  $w_p(r_p)$  of the  $M_{0.1r} < -21$  sample to the model prediction for parameter values  $M_1 = 4.74 \times 10^{13} h^{-1} M_\odot$  and  $\alpha = 0.89$ . These values are determined by a maximum-likelihood fit to the data points incorporating the covariance matrix derived from the mock catalogs. Matching the observed number density of the sample requires  $M_{\min} = 6.10 \times 10^{12} h^{-1} M_\odot$ , and the fraction of galaxies in halos with  $M < M_1$  is 75%. The  $\chi^2$  value of the fit is 9.3 for 10 degrees of freedom (12 data points minus the 2 parameters that are varied to fit the correlation function), or  $\chi^2/\text{d.o.f.} = 0.93$ . Thus, the HOD model yields a statistically acceptable fit to the data, and with the same number of free parameters as the power law, it fits the data significantly better ( $\Delta\chi^2 = 51.9$ ). The lower panel of Figure 3 shows the ratio of the data points and the HOD model to the best-fit power law, from which one can see that the model predicts just the sort of dip at  $\sim 1-2 h^{-1} \text{ Mpc}$  and bulge at several  $h^{-1} \text{ Mpc}$  that is observed in the data.

The error bars on the model parameters (defined by  $\Delta\chi^2 = 1$ ) are  $\pm 0.05$  in  $\alpha$  and  $\pm (0.5 \times 10^{13} h^{-1} M_\odot)$  in  $M_1$ . These errors are strongly correlated, but the mean occupation at  $M = 10^{14.5} h^{-1} M_\odot$  is constrained to  $\log_{10}\langle N_{14.5} \rangle = 0.733 \pm 0.007$ , with an error that is nearly uncorrelated with  $\alpha$ . If we use the jackknife covariance matrix estimated from the data instead of the mock catalog covariance matrix, we obtain a very similar fit with nearly the same  $\chi^2$ . If we use the mock catalog covariances without the scaling described in §2, we obtain a very similar fit with a lower  $\chi^2$ . A mean multiplicity of 5.4 at  $10^{14.5} h^{-1} M_\odot$  might look low at first glance, but our luminosity

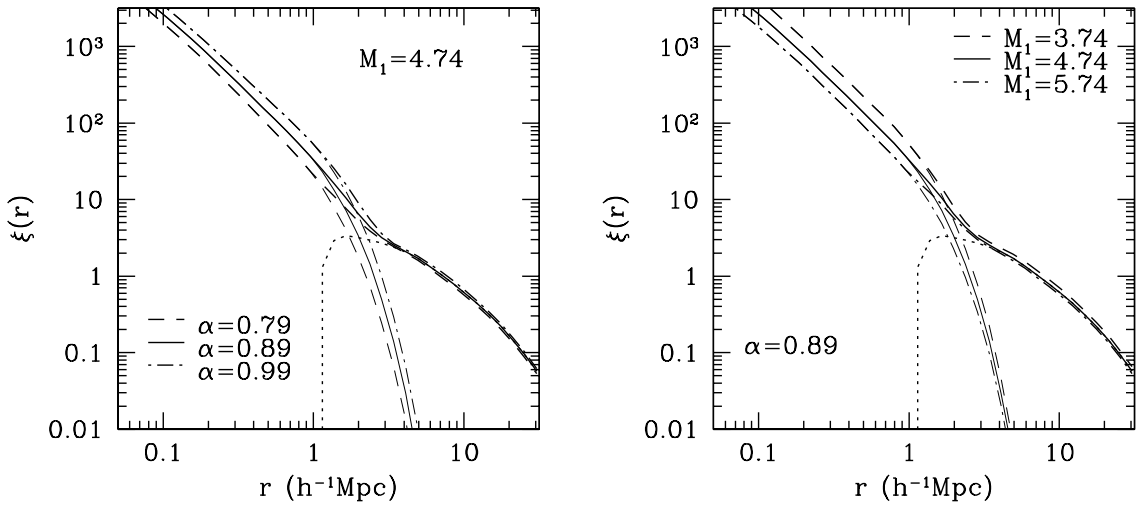


Fig. 2.— Real space galaxy correlation functions for HOD models with  $M_1 = 4.74 \times 10^{13} h^{-1} M_\odot$  and varying values of  $\alpha$  (left), and for  $\alpha = 0.89$  and varying values of  $M_1$  (right). For each model we plot the total  $\xi(r)$  (upper curves) and the 1-halo contribution (lower curves). The dotted curve shows the 2-halo contribution for the central model; this contribution is similar but not identical in the other models. In all models, the parameter  $M_{\min}$  is adjusted to keep the space density fixed at  $n = 9.9 \times 10^{-4} h^3 \text{Mpc}^{-3}$ .

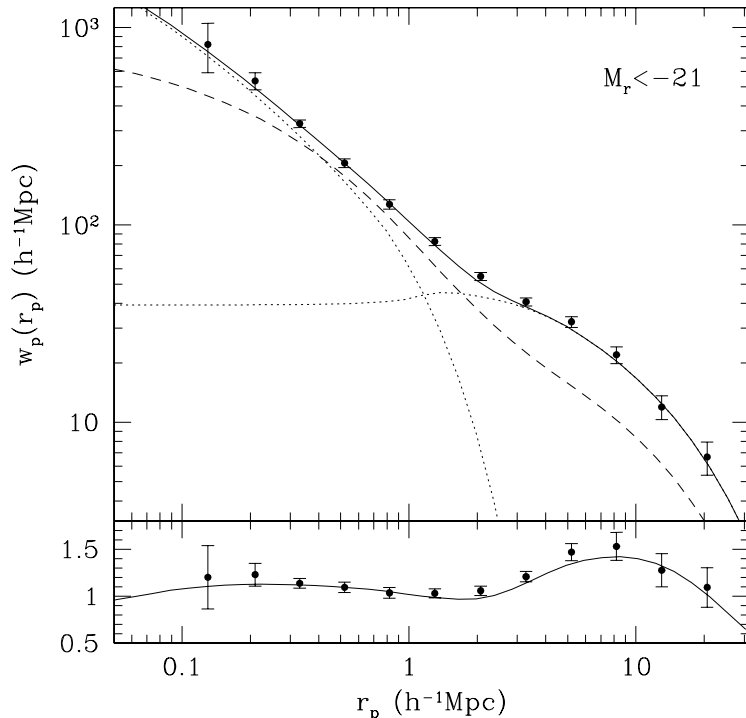


Fig. 3.— Projected correlation function for the  $M_{0.1r} < -21$  sample together with the predicted correlation function for the best-fit HOD model, with parameters  $\alpha = 0.89$ ,  $M_1 = 4.74 \times 10^{13} h^{-1} M_\odot$ , and  $M_{\min} = 6.10 \times 10^{12} h^{-1} M_\odot$ . The reduced  $\chi^2$  for this 2-parameter fit is  $\chi^2/\text{d.o.f.} = 0.93$ , while the reduced  $\chi^2$  for the power-law fit shown by the solid line in Figure 1 is  $\chi^2/\text{d.o.f.} = 6.12$ . The lower panel shows the data and model prediction divided by this best-fit power law. In the upper panel, dotted curves show the 1-halo and 2-halo contributions to  $w_p(r_p)$  and the dashed curve shows the projected correlation function for the matter computed from the nonlinear power spectrum of Smith et al. (2003).

threshold is fairly high ( $\sim 1.5L_*$ ), and this multiplicity is reasonably consistent with the number of comparably luminous galaxies in Virgo (Trentham & Tully 2002) and with the measured richness or luminosity of SDSS clusters at a similar cumulative space density of  $n(> M) = 6.4 \times 10^{-6} h^3 \text{Mpc}^{-3}$  (Bahcall et al. 2003).

The HOD model that we have fit to the data is not unique, since we could have adopted a different form for  $\langle N \rangle_M$ , or for the width of the distribution at fixed  $M$ , or for the internal distribution of galaxies within halos. For example, if we change the normalization of the  $c(M)$  relation from  $c(M_*) = 11$  to 20 or 5, or the index from  $-0.13$  to 0 or  $-0.25$ , then we still get acceptable (though slightly worse) fits to the  $w_p(r_p)$  data, but with changes  $\sim 0.1$  in  $\alpha$  and associated changes in  $M_1$  and  $M_{\min}$ . Increasing halo concentrations shifts 1-halo pairs towards smaller separations, and this change can be compensated by putting more galaxies into halos with large virial radii. We have also considered a model for  $P(N|\langle N \rangle)$  that closely tracks the predictions of semi-analytic models and SPH simulations (Kauffmann et al. 1999; Benson et al. 2000; Seljak 2000; Scoccimarro et al. 2001; Berlind et al. 2003), in which the width climbs steadily from nearest-integer at  $\langle N \rangle \sim 1$  to Poisson at high  $N$ , with the transition halfway complete at  $\langle N \rangle \sim 4$ . We again find that we can fit the data nearly as well as with our baseline model, with only slight changes to the  $\langle N \rangle_M$  parameters. We are also able to fit  $w_p(r_p)$  well using Kravtsov et al.’s (2004) proposed parameterization of a step-function  $\langle N \rangle_M$  for central galaxies and a power-law  $\langle N \rangle_M$  for satellites, instead of the plateau/power-law form for the full population that we adopt here.

The most important lesson to be learned from these alternative fits is that all of them produce a very similar  $w_p(r_p)$ , with an inflection at  $r_p \sim 1 - 2 h^{-1} \text{ Mpc}$  that always marks the transition from the 1-halo regime of the correlation function to the 2-halo regime. Thus, this interpretation of the observed feature in  $w_p(r_p)$  is not sensitive to the details of our HOD model or our calculational method. Our account parallels Seljak’s (2000) proposed explanation of the inflection in the observed galaxy power spectrum (Peacock 1997). We have not examined alternative cosmological parameter choices because our analytic approximation is calibrated against a specific N-body simulation, but we anticipate that modest changes in the normalization  $\sigma_8$  would still allow successful fits to  $w_p(r_p)$ , with compensating changes in  $\langle N \rangle_M$ . Substantial changes to the shape of the matter power spectrum, on the other hand, might be impossible to accommodate.

We have also investigated a model in which the distribution  $P(N|\langle N \rangle)$  is Poisson instead of nearest-integer, and in this case we can find no combination of  $M_1$  and  $\alpha$  that comes close to fitting the  $w_p(r_p)$  data. Thus, we confirm earlier arguments that the sub-Poisson fluctuations predicted by the leading galaxy formation models are essential to reproducing observed galaxy clustering.

Gaztañaga & Juszkiewicz (2001) have also discussed deviations from a power-law correlation function, based on the real space  $\xi(r)$  that Baugh (1996; see also Padilla & Baugh 2003) obtained by inverting the angular clustering measurements from the Automatic Plate Measuring (APM) galaxy catalog (Maddox et al. 1990). The inflection point in the inverted APM  $\xi(r)$  occurs at  $r \approx 5 h^{-1} \text{ Mpc}$ , which is larger than the scale of  $r_p \approx 2 h^{-1} \text{ Mpc}$  where we find an inflection

in  $w_p(r_p)$ . We have not attempted to invert  $w_p(r_p)$  to derive  $\xi(r)$  directly, but the real space correlation function of the best fitting HOD model changes slope most rapidly between 2 and  $4 h^{-1}$  Mpc (Figure 2). Our methods are different, and a quantitative assessment of the discrepancy is difficult, so while the scale of the feature we find appears to be somewhat smaller, it is not clear that the APM and SDSS results are incompatible.

Gaztañaga & Juszkiewicz (2001) argue that the inflection of  $\xi(r)$  is connected to the onset of non-linear gravitational evolution, drawing on the pair conservation equation (Davis & Peebles 1977), and they conclude that the coincidence of this inflection scale with the galaxy correlation length implies that APM galaxies trace the underlying mass distribution to a good approximation. We associate the feature in  $w_p(r_p)$  with the transition from the 2-halo regime of the correlation function to the 1-halo regime, at a smaller, more highly nonlinear scale set by the virial diameters of rare, massive halos. Gaztañaga & Juszkiewicz (2001) model the APM data using N-body simulations by Baugh & Gaztañaga (1996) that have an initial power spectrum custom designed to evolve into the observed APM power spectrum (using the methods of Peacock & Dodds [1994] and Jain, Mo, & White [1995]). We have assumed instead that the underlying matter correlation function, shown by the dashed line in Figure 3, is that of a  $\Lambda$ CDM cosmological model with parameters favored by other observations. The correlation function of the  $M_{0.1r} < -21$  galaxies is biased by a factor  $b^2 \sim 2$  on large scales, and the bias is strongly scale-dependent in the non-linear regime. Figure 4 plots the ratio  $[\xi_{gg}(r)/\xi_{mm}(r)]^{1/2}$  for our best-fit model, which is similar in shape to the “bias function” that Jenkins et al. (1998) concluded would be required to reconcile CDM predictions with observations. While the scale dependence is itself complex, it emerges from a simple HOD model with two free parameters that is motivated by the predictions of contemporary galaxy formation theory. A strict mass-traces-light model, on the other hand, must choose a full 1-dimensional function, the initial power spectrum, specifically to match the observed correlation function, and this function has no motivation from theory or other observations. Tests of our model will soon be provided by additional clustering measurements such as the group multiplicity function, higher order correlation functions, and dynamical group masses.

We have concentrated in this paper on the clustering of relatively luminous galaxies, and these exhibit stronger departures from a power-law correlation function than lower luminosity populations. In fact, hydrodynamic simulations and semi-analytic models predict just this behavior: departures from a power law are stronger for luminous, rare, strongly clustered galaxies than for lower luminosity populations of higher space density and lower clustering amplitude (Weinberg et al. 2004; Berlind et al. 2003). However, as noted above, we find similar signatures of the 1-halo to 2-halo transition in most of the other SDSS volume-limited samples we have analyzed, albeit at lower significance. We consistently find that HOD models of the sort developed here can fit the measured correlation functions as well as or better than power laws. We will present these results and their implications for the luminosity dependence of galaxy halo occupations elsewhere (I. Zehavi et al., in preparation). As noted in §2, Hawkins et al. (2003) find small deviations from a power-law correlation function, similar to those found here, in their analysis of the full,

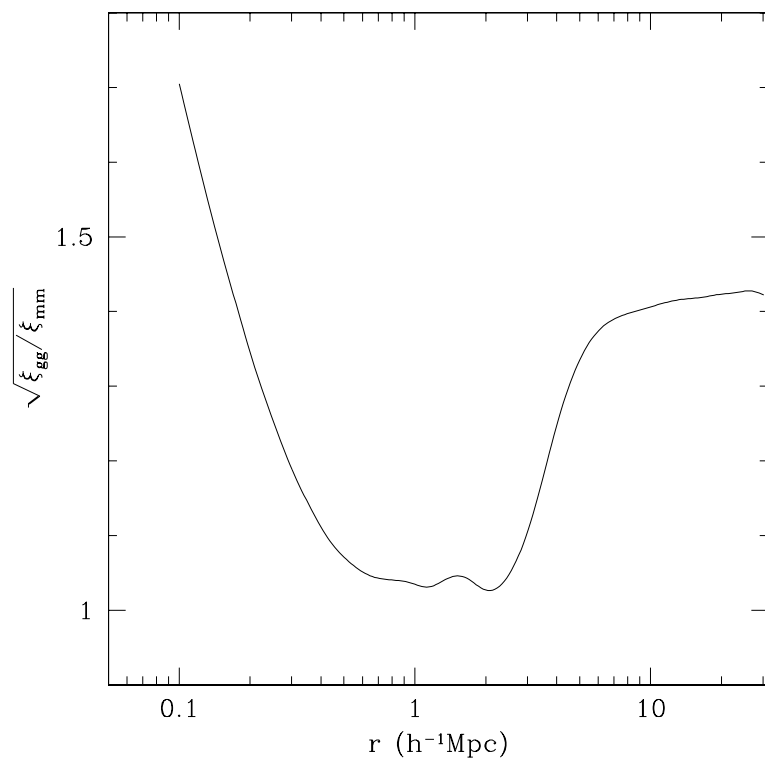


Fig. 4.— “Bias function” defined by  $b(r) = [\xi_{gg}(r)/\xi_{mm}(r)]^{1/2}$  for the best-fit HOD model, where  $\xi_{mm}(r)$  is the non-linear matter correlation function for our adopted cosmology.

flux-limited 2dFGRS. The existence of similar features in independent analyses of the two largest galaxy redshift surveys demonstrates their robustness, and the modeling presented here shows that they are physically natural.

The parameters of power-law fits to the galaxy correlation function have long been an important constraint on cosmological parameters and galaxy formation models. We anticipate, however, that  $w_p(r_p)$  measurements of increasing precision will reveal departures from a power-law that are increasingly significant, for a variety of galaxy classes. These departures encode information about the number of galaxies as a function of halo mass, about the distribution of halo virial radii, and about the relative distributions of galaxies and dark matter within halos. We therefore expect that future measurements of the galaxy correlation function will yield ever richer information about cosmology and galaxy formation.

We thank Chris Miller, Ryan Scranton, and Michael Strauss for helpful discussions and comments. Support for the analyses in this paper was provided by NSF grants AST00-98584 and PHY-0079251.

Funding for the creation and distribution of the SDSS Archive has been provided by the Alfred P. Sloan Foundation, the Participating Institutions, the National Aeronautics and Space Administration, the National Science Foundation, the U.S. Department of Energy, the Japanese Monbukagakusho, and the Max Planck Society. The SDSS Web site is <http://www.sdss.org/>.

The SDSS is managed by the Astrophysical Research Consortium (ARC) for the Participating Institutions. The Participating Institutions are The University of Chicago, Fermilab, the Institute for Advanced Study, the Japan Participation Group, The Johns Hopkins University, Los Alamos National Laboratory, the Max-Planck-Institute for Astronomy (MPIA), the Max-Planck-Institute for Astrophysics (MPA), New Mexico State University, University of Pittsburgh, Princeton University, the United States Naval Observatory, and the University of Washington.

### A. Accuracy of the Analytic Approximation

We have used the GIF  $\Lambda$ CDM N-body simulation of Jenkins et al. (1998) to guide the development of our analytic model for the correlation function and to test its accuracy. Figure 5 presents an example of such a test, for an HOD model similar to the best-fit baseline model described in §4. We identify halos in the GIF simulation using a friends-of-friends algorithm (Davis et al. 1985) with linking parameter of 0.2, which selects systems of overdensity  $\rho/\bar{\rho} \sim 200$ . We choose the number of galaxies in each halo based on the model  $P(N|M)$ , place the first galaxy at the halo center, and choose random dark matter particles within the halo for other galaxies. Points show  $\xi(r)$  for this galaxy population, with  $1\sigma$  error bars estimated by jackknife resampling of the eight octants of the  $141.3 h^{-1}$  Mpc simulation cube. The solid curve shows the analytic model prediction for the same HOD. It lies systematically above the numerical results at large  $r$  because of the truncation

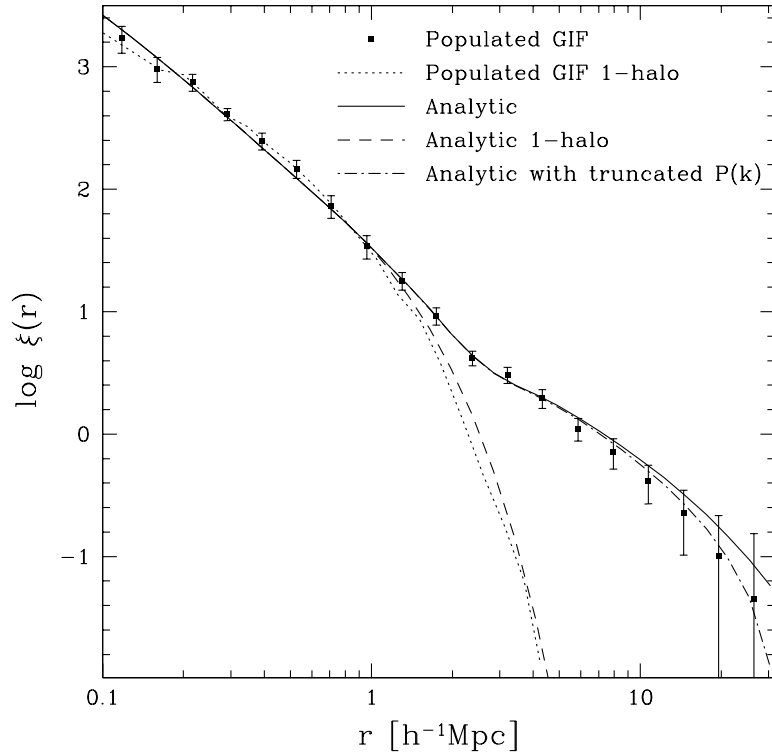


Fig. 5.— Test of the analytic correlation function model against the GIF N-body simulation of Jenkins et al. (1998). Friends-of-friends halos in the GIF simulation are populated using an HOD model like the one that best fits the SDSS  $M_{0.1r} < -21$  data. Points show the numerical results with jackknife error bars, and the dotted line shows the 1-halo contribution alone. The solid line shows the full analytic model prediction, with the dashed line indicating the 1-halo term. The dot-dashed line shows the effect of truncating  $P(k)$  at the size of the simulation cube when computing the analytic prediction.

of large scale power on the scale of the simulation box. When this truncation is incorporated into the analytic calculation (dot-dashed curve), the falloff of  $\xi(r)$  at large  $r$  is well reproduced. Dotted and dashed curves show the 1-halo contributions from the simulation and the analytic model, respectively. The analytic 1-halo term extends slightly further than the numerical one, probably because of the absence of very high mass halos in the finite simulation volume.

From this comparison, we conclude that the analytic model is accurate to the degree that we are able to test it with this simulation. This test implies that our treatment of scale-dependent halo bias and halo exclusion (see §3) is adequate for our present purposes. Residual inaccuracies of  $\sim 10\text{--}20\%$  could still be present at some separations. When it comes to fitting the data, inaccuracies at this level could have a noticeable effect on our determinations of best-fit HOD parameters, but their effect is comparable to that of changes in the halo  $c(M)$  relation discussed in §4, and they are unlikely to change our conclusions about the physical significance of the departures from a power-law  $w_p(r_p)$ . We have chosen to base our fits on a numerically calibrated analytic model rather than the populated GIF simulation itself for several reasons: the analytic approach provides us with a well defined model that is not tied to the numerical details of a particular simulation, it is more practical for maximum-likelihood parameter determinations, and it is not affected by truncation of large scale power. Because  $w_p(r_p)$  is defined by integrating  $\xi(r_p, \pi)$  out to large separations, the effect of this missing power is greater than that in Figure 5, depressing  $w_p(r_p)$  by factors of 1.5–2 at  $r_p = 10\text{--}20 h^{-1}$  Mpc. The analytic model can in principle be applied to other cosmological models, but we have not yet tested our form of the scale-dependent halo bias factor on other simulations, so we do not know if it remains accurate for other cosmological parameters. Sheth & Lemson (1999) and Casas-Miranda et al. (2002) discuss general expectations for the scale-dependence of halo bias.

## REFERENCES

Bahcall, N. A. et al. 2003, ApJS, 148, 243

Baugh, C. M. 1996, MNRAS, 280, 267

Baugh, C. M. & Gaztañaga, E. 1996, MNRAS, 280, L37

Benson, A. J., Cole, S., Frenk, C. S., Baugh, C. M., & Lacey, C. G. 2000, MNRAS, 311, 793

Berlind, A. A., & Weinberg, D. H. 2002, ApJ, 575, 587

Berlind, A. A., Weinberg, D. H., Benson, A. J., Baugh, C. M., Cole, S., Davé, R., Frenk, C. S., Jenkins, A., Katz, N., & Lacey, C. G. 2003, ApJ, 593, 1

Blanton, M.R., Lupton, R.H., Maley, F.M., Young, N., Zehavi, I., & Loveday, J. 2003a, AJ, 125, 2276

Blanton, M. R. et al. 2003b, AJ, 125, 2348

Blanton, M. R. et al. 2003c, *ApJ*, 592, 819

Bullock, J. S., Kolatt, T. S., Sigad, Y., Somerville, R. S., Kravtsov, A. V., Klypin, A. A., Primack, J. R., & Dekel, A. 2001, *MNRAS*, 321, 559

Calzetti, D., Giavalisco, M., & Meiksin, A. 1992, *ApJ*, 398, 429

Casas-Miranda, R., Mo, H. J., Sheth, R. K., & Boerner, G. 2002, *MNRAS*, 333, 730

Cen, R. & Ostriker, J. P. 2000, *ApJ*, 538, 83

Colín, P., Klypin, A. A., Kravtsov, A. V., & Khokhlov, A. M. 1999, *ApJ*, 523, 32

Connolly, A., et al. 2002, *ApJ*, 579, 42

Davis, M., Efstathiou, G., Frenk, C. S., & White, S. D. M. 1985, *ApJ*, 292, 371

Davis, M., & Peebles, P. J. E. 1977, *ApJS*, 34, 425

Davis, M., & Peebles, P. J. E. 1983, *ApJ*, 267, 465

Dekel, A., & Aarseth, S. J. 1984, *ApJ*, 283, 1

Efstathiou, G., Bond, J. R., & White, S. D. M. 1992, *MNRAS*, 258, 1p

Eisenstein, D. J. et al. 2001, *AJ*, 122, 2267

Fisher, K.B., Davis, M., Strauss, M.A., Yahil, A., & Huchra, J.P. 1994, *MNRAS*, 266, 50

Fukugita, M., Ichikawa, T., Gunn, J. E., Doi, M., Shimasaku, K., & Schneider, D. P. 1996, *AJ*, 111, 1748

Gaztañaga, E. & Juszkiewicz, R. 2001, *ApJ*, 558, L1

Gaztañaga, E. 2002, *ApJ*, 580, 144

Gott, J. R. & Turner, E. L. 1979, *ApJ*, 232, L79

Groth, E. J. & Peebles, P. J. E. 1977, *ApJ*, 217, 385

Gunn, J. E., et al. 1998, *AJ*, 116, 3040

Guzzo, L., Iovino, A., Chincarini, G., Giovanelli, R., & Haynes, M. P. 1991, *ApJ*, 382, L5

Hamilton, A. J. S. & Tegmark, M. 2002, *MNRAS*, 330, 506

Hawkins, E., et al. 2003, *MNRAS*, 346, 78

Hogg, D.W., Schlegel, D.J., Finkbeiner, D.P., & Gunn, J.E. 2001, *AJ*, 122, 2129

Jain, B., Mo, H. J., & White, S. D. M. 1995, MNRAS, 276, L25

Jenkins, A., Frenk, C. S., Pearce, F. R., Thomas, P. A., Colberg, J. M., White, S. D. M., Couchman, H. M. P., Peacock, J. A., & Efstathiou, G., & Nelson, A. H. 1998, ApJ, 499, 20

Jenkins, A., Frenk, C. S., White, S. D. M., Colberg, J. M., Cole, S., Evrard, A. E. Couchman, H. M. P., & Yoshida, N. 2001, MNRAS, 321, 372

Jing, Y. P., Börner, G., & Suto, Y. 2002, ApJ, 564, 15

Jing, Y. P., Mo, H. J., & Börner, G. 1998, ApJ, 494, 1

Kauffmann, G., Nusser, A., & Steinmetz, M. 1997, MNRAS, 286, 795

Kauffmann, G., Colberg, J. M., Diaferio, A., & White, S. D. M. 1999, MNRAS, 303, 188

Kravtsov, A. V., Berlind, A. A., Wechsler, R. H., Klypin, A. A., Gottloeber, S., Allgood, B., & Primack, J. R. 2004, ApJ, in press, astro-ph/0308519

Landy, S. D. & Szalay, A. S. 1993, ApJ, 412, 64

Lupton, R., Gunn, J. E., Ivezić, Z., Knapp, G. R., Kent, S., & Yasuda, N. 2001, in ASP Conf. Ser. 238, Astronomical Data Analysis Software and Systems X, ed. F. R. Harnden, Jr., F. A. Primini, and H. E. Payne (San Francisco: Astr. Soc. Pac.), p. 269, astro-ph/0101420

Ma, C., & Fry, J. N. 2000, ApJ, 543, 503

Maddox, S. J., Efstathiou, G., Sutherland, W. J., & Loveday, J. 1990, MNRAS, 242, L43

Magliocchetti, M. & Porciani, C. 2003, MNRAS, 346, 186

Marzke, R. O., Geller, M. J., da Costa, L. N., & Huchra, J. P. 1995, AJ, 110, 477

Mo, H.J., & White S.D.M. 1996, MNRAS, 282, 347

Navarro, J., Frenk, C. S., & White, S. D. M. 1996, ApJ, 462, 563

Norberg, P., et al. 2001, MNRAS, 328, 64

Padilla, N. D. & Baugh, C. M. 2003, MNRAS, 343, 796

Peacock, J. A. 1997, MNRAS, 284, 885

Peacock, J. A., & Dodds, S. J. 1994, MNRAS, 267, 1020

Peacock, J. A., & Smith, R. E. 2000, MNRAS, 318, 1144

Pearce, F. R., Jenkins, A., Frenk, C. S., Colberg, J. M., White, S. D. M., Thomas, P. A., Couchman, H. M. P., Peacock, J. A., & Efstathiou, G. 1999, ApJ, 521, L99

Peebles, P. J. E. 1974, A&A, 32, 197

Percival, W. J., et al. 2001, MNRAS, 327, 129

Pier, J.R., Munn, J.A., Hindsley, R.B., Hennessy, G.S., Kent, S.M., Lupton, R.H., & Ivezić, Z. 2003, AJ, 125, 1559

Press, W. H., & Schechter, P. 1974, ApJ, 187, 425

Schechter, P. 1976, ApJ, 203, 297

Scoccimarro, R., & Sheth, R. K. 2002, MNRAS, 329, 629

Scoccimarro, R., Sheth, R. K., Hui, L., & Jain, B. 2001, ApJ, 546, 20

Seljak, U. 2000, MNRAS, 318, 203

Sheth, R. K., & Lemson, G. 1999, MNRAS, 305, 946

Sheth, R. K., Mo, H. J., & Tormen, G. 2001, MNRAS, 323, 1

Smith, J. A. et al. 2002, AJ, 123, 2121

Smith, R. E. et al. 2003, MNRAS, 341, 1311

Somerville, R. S., Lemson, G., Sigad, Y., Dekel, A., Kauffmann, G., & White, S. D. M. 2001, MNRAS, 320, 289

Stoughton, C. et al. 2002, AJ, 123, 485

Strauss, M.A., et al. 2002, AJ, 124, 1810

Takada, M. & Jain, B. 2003, MNRAS, 340, 850

Tegmark, M et al. 2004, ApJ, 606, 702

Totsuji, H. & Kihara, T. 1969, PASJ, 21, 221

Trentham, N. & Tully, R. B. 2002, MNRAS, 335, 712

van den Bosch, F. C., Mo, H. J., & Yang, X. 2003, MNRAS, 340, 771

Weinberg, D. H., Davé, R., Katz, N., & Hernquist, L. 2004, ApJ, 601, 1

White, M., Hernquist, L., & Springel, V. 2001, ApJ, 550, L129

Yang, X., Mo, H. J., & van den Bosch, F. C. 2003, MNRAS, 339, 1057

York, D. G. et al. 2000, AJ, 120, 1579

Yoshikawa, K., Taruya, A., Jing, Y. P., Suto, Y. 2001, ApJ, 558, 520

Zehavi, I. et al. 2002, ApJ, 571, 172